https://doi.org/10.1016/j.conbuildmat.2021.123522

Numerical investigation on the influence of microstructure evolution of bitumen on its micromechanical property

Cong Du[a], Guoyang Lu[b], Kaloyan Ganchev[a], Pengfei Liu[a, 1], Markus Oeser[a]

[a] *Institute of Highway Engineering, RWTH Aachen University, Aachen, Germany*

[b] *Department of Civil and Environmental Engineering, The Hong Kong Polytechnic University, Hong Kong, China*

Abstract:

The variation of microstructures of the bitumen due to changes in chemical composition has been found during construction and its service life period, such as aging and rejuvenation processes. The microstructure variation plays an essential role in the micromechanical performance of the bitumen and thus in the mechanical behavior of asphalt mixtures. This research aimed to reveal the influence of microstructure changes of bitumen on its micromechanical responses. Based on the atomic force microscopy (AFM) technology, the microstructure (bee structures) of the bitumen can be detected. With the self-developed microstructural finite element (FE) models, the micromechanical responses of bitumen with different bee structures were developed and simulated. The result shows that the computational load-bearing capacity of the bitumen increases with the increase of the peri phase content, but the difference is not significant. The development of high stresses within bee phase is mainly because of the inhomogeneity of material. Additionally, the distribution of the tensile strain becomes more homogeneous with the increase of the peri phase content. This research indicates that the ability to manipulate the microstructure of bitumen contributes to establishing a better understanding of the relationship between the chemical composition of the bitumen and its microstructure, and further investigating the effects, such as the aging and rejuvenation, on the micromechanical performance of bitumen.

Keywords: Bitumen; Micromechanical property; Microstructure variation; AFM technology; FE simulation

1 Corresponding Author: Pengfei Liu, Dr.-Ing., Tel: +49-241-8020389, Fax: +49-241-8022141; Email: liu@isac.rwth-aachen.de

1 Introduction

Acting as binding materials of asphalt mixture, bitumen plays the most significant role in asphalt mixtures despite constituting the minor percentage, which is supplying consistency to the overall materials, improving the driving comfort and flexible maintenance of asphalt pavements, etc. [1-3]. Numerous studies have conducted laboratory macroscale tests to characterize the rheological properties of bitumen, and the results indicated that the performances of the bitumen were related to their chemical components [4-6]. Two typical processes can change the chemical components of the bitumen: aging and rejuvenation. Several factors including light, heat, oxygen, and water can cause the aging of bitumen, which reduces the penetration and ductility and improves the softening point and breaking point of bitumen [7, 8]. The rejuvenation of the aged bitumen, as a remedy, plays an essential role in rehabilitating the aged bitumen and producing the low-cost and environmental-friendly alternatives for asphalt binders and asphalt mixtures [9-13].

In order to seek a deeper understanding of the complex mechanism relating to the changes of the chemical components due to aging and rejuvenating of bitumen, technological advancement such as atomic force microscopy (AFM) has greatly facilitated researchers in examining bitumen at the microscale. The AFM employs a sharp tip, which is only several micro lengths and located at the free end of a cantilever, probes the surface of the bitumen while collecting data [14]. The microstructure of the bitumen surface can be mapped according to the displacement of the tip [14, 15]. Loeber et al. [16] studied the microstructure of bitumen using the AFM and Scanning Electron Microscope (SEM), and the surface morphology of bitumen can be visualized. Three distinct phases were observed in the microstructure of the bitumen based on the AFM images. The first phase can be described as the ‘bee’ phase, a second phase that surrounds the ‘bee’ phase is referred to as the ‘peri’ phase and a third phase is referred to as the ‘interstitial phase’ that occupies the space between the peri phase [17].

The bee structure was firstly characterized by Loeber et al. [16], and was believed to closely relate to the asphaltene content. Recent research by Ramm et al. [18] had found that the bee structures

are thin film that relates to the crystallizable fractions of the binder. Despite that the bee structures were found to be different from the internal bulk microstructure of the bitumen in their sizes and morphologies, Ramm et al. [19, 20] also reported that they might have similar chemical components since both the two structures formed at similar temperatures. Researches from Lyne et al. [21, 22] found that the bee and peri phases have higher Young's modulus than the interstitial phase. Allen et al. [23, 24] evaluated the chemistry and rheology of the microstructure within bitumen and their influence on the macroscopic properties, and found that the bee structures might serve as the critical positions for crack nucleation. In addition, Holleran et al. [25] found strong correlations between the elastic modulus of bee structure and the rheological properties of bitumen, which indicates that the bee structures might represent the bulk properties of binders. Yang et al. [26] used the AFM peak force quantitative nano-mechanical mapping mode to investigate the micromechanical properties of the aged bitumen, and the bee structures are found to have close relationship with the penetration grade. Cavalli et al. [27] employed the AFM to gain a better understanding of the microstructural morphology of the rejuvenated bitumen. Within the results, the formation of the bee phase contributes to the increase of the surface's moduli. By comprehensively investigating the researches from Guo et al. [17], Das et al. [28], Chen et al. [29] and Ganter et al. [30], the bee phases of the bitumen are found to become more remarkable after being subjected to the aging processes including the rolling thin film oven test (RTFOT) and pressure aging vessel (PAV); furthermore, rejuvenators significantly reduced the bee phase of the aged bitumen.

Although the importance of the microstructure (bee, peri phase, interstitial) of bitumen was identified in the past, very little research has been made towards the relationships between the microstructure feature and the micromechanical responses of the bitumen. The image-based FE simulation shows powerful abilities in modeling and calculating the mechanical responses of the heterogeneous materials with consideration of their internal structure characteristics. Based on the digital image processing (DIP) technology, the multiple phases of materials can be precisely captured

and the heterogeneous models can be established. In recent years, numerical attempts were used towards the stress and strain responses of asphaltic materials at microscale and mesoscale. Sun et al. [31] established the two-dimensional model of asphalt mixtures to investigate the damage performance of asphalt pavement, in which the multiscale approach was employed. Liu et al. [32] investigated the relationship between the inner structure and mechanical performance of asphalt mixtures with different compaction degrees. To improve the understanding of the fracture mechanism of asphalt pavement, Kollmann et al. [33] incorporated the X-ray computed tomography (X-ray CT) technology and the FE mesoscale model to simulate the indirect tensile test (IDT), and the results showed that the temperature and air void content have significant effects on the fracture behavior. The abovementioned researches provided reasonable approaches to deeply analyze the structural feature and mechanical properties of asphalt mixtures; however, the investigation on the mechanism of such mechanical behavior within bitumen requires relatively smaller scales and high precision techniques. Fortunately, in cooperation with the AFM mapping technology, the numerical simulation enables researchers to effectively investigate the micromechanical properties of bitumen with respect to its microstructure evolution due to the change of chemical components. One of such researches was conducted by Jahangir et al. [34], they correlated the microstructure and micromechanics of two different virgin bitumen by combining the AFM and finite element（FE） simulations, and the localized stress or strain were clearly exhibited, which relates to the damage nucleation and propagation.

Based on the research from Jahangir et al. [34], the objective of this study is to reveal the influence of microstructure changes of bitumen on its micromechanical responses. Using the AFM technology and FE simulation performed in general purpose FE software ABAQUS, the micromechanical responses of bitumen with different bee structures were computed, and the relationship between the microstructure changes of bitumen and its micromechanical responses was identified and discussed. Therefore, the proposed study can precisely capture the micromechanical

performance of bitumen by artificially manufacturing the phase areas of the bee-structures, and hence can reveal the mechanism of the microstructure variation on bitumen. However, the model parameters for the bee structure were determined as linear elastic based on the DMT modulus, and further researches related to the viscoelastic properties of the bitumen should be conducted.

2 Development of FE models with different microstructural phases

The bitumen with a penetration grade of 80/100 was selected from the literature [35], which is used as a Paving Grade Bitumen for the construction of asphalt pavement with superior properties. The properties of this material can be seen in **Table 1**.

Table 1: Chemical composition of the bitumen sample

Parameter	Value
Penetration at 25°C [1/10mm]	81
R&B softening point [°C]	45.0
Dynamic viscosity at 60°C (Pa.s)	181
Density at 15°C (g/cm^3)	1.010

By studying the bitumen sample using AFM, a variety of properties can be obtained such as modulus, adhesion, dissipation, and deformation. The details about the test using AFM can be found from the literature [17]. To identify and separate the different phases of the bitumen in the image derived from the AFM, the DIP techniques were applied. In the DIP method, the images of bitumen samples from AFM were read into the MATLAB image processing toolbox, and different phases of the bitumen were separated based on the different gray scales of the images. Because of different properties of material adhesion, the phases of the bitumen in the AFM image presented different gray values, i.e., the bee phase resulted in the maximum gray values while interstitial returned the minimum. Subsequently, the binary images of different phases were established by employing appropriate gray threshold, and their boundaries were extracted. According to the coordinates of the boundaries, the microstructure of the bitumen was reconstructed using the FE software ABAQUS. The original image derived from AFM and the separate phases of the bitumen are shown in Figure 1~~Figure 1~~,

Formatted: Font color: Auto
Formatted: Font color: Auto
Formatted: Font color: Auto
Formatted: Font color: Auto
Formatted: Font color: Auto
Formatted: Font color: Auto
Formatted: Font color: Auto
Formatted: Font color: Auto
Formatted: Font: 12 pt
Formatted: Font: 12 pt, Not Italic

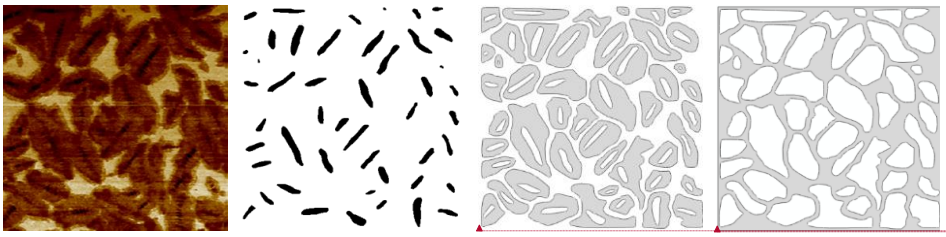

(a) (b) (c) (d)

Figure 1: Images of (a) bitumen sample acquired from AFM; (b) bee; (c) peri phase; (d) interstitial

This geometry information was input to ABAQUS for the construction of the FE model with different phases. As aforementioned, during the aging and rejuvenation processes on the bitumen, the contents of bee and peri phase are changed [17, 28-30]. According to their investigations, this study assumed that the peri phase will be transferred into bee phases in the aging process, and the rejuvenation process was assumed to have the reverse effects to the aging. Therefore, in this study, four FE models with different bee and peri phase contents are created to account for the aged and rejuvenated bitumen, and further to investigate the effect of the microstructure evolution on the micro-mechanical properties of the bitumen. The aging and rejuvenation of the bitumen are two of typical processes which cause microstructure evolution (change of the chemical components) of the bitumen. However, it is worth noting that the methodology of this study can also be applied to investigate the microstructure evolution of the bitumen during other processes.

The base bitumen shown in Figure 1~~Figure 1~~ contains the contents of 61.3% peri phase and 8.9% bee, which was created according to the AFM image and DIP technology. Based on the model of the base bitumen, one FE model with less content of the peri phase (51.3%) and more content of the bee (11.4%) was created to consider the aging effect on the bitumen; two more FE models were created to simulate the microstructure of the bitumen influenced by the rejuvenator, in which the content of the peri phase was increased to 71.3% and 81.3%, and the content of bee was decreased to 6.4% and 3.9%. The four models are shown in Figure 2~~Figure 2~~,

Formatted: Font color: Auto
Formatted: Font color: Auto
Formatted: Font color: Auto
Formatted: Font color: Auto
Formatted: Font color: Auto
Formatted: Font: 12 pt
Formatted: Font: 12 pt, Not Italic
Formatted: Font color: Auto
Formatted: Font color: Auto
Formatted: Font color: Auto
Formatted: Font color: Auto
Formatted: Font: 12 pt
Formatted: Font: 12 pt, Not Italic

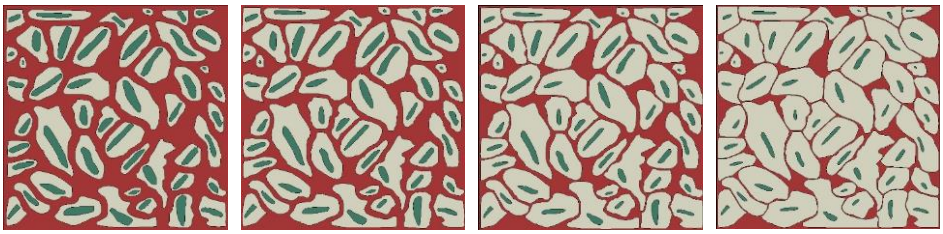

(a) (b) (c) (d)

Figure 2: FE Models with different microstructural phases (a) peri phase 51.3% and bee 11.4%; (b) peri phase 61.3% and bee 8.9%; (c) peri phase 71.3% and bee 6.4%; (d) peri phase 81.3% and bee 3.9%

In the FE models, the different phases were then tied together, i.e., the micro-crack was not considered in the simulation. The FE models of the bitumen were discretized by linear triangle 3-node plane stress elements (CPS3). In order to examine the effect of applied load/displacement on the microstructure of bitumen, a displacement with a constant loading rate of 1.5 μm/s was applied to the upper edge of the test specimen for 1 second. Meanwhile, the bottom edge of the test specimen was fixed. One 2D assembled model with the boundary condition is shown in Figure 3~~Figure 3~~ (a). The FE meshes along with the corresponding phases can be seen in Figure 3~~Figure 3~~ (b).

Formatted: Font color: Auto

Formatted: Font color: Auto

Formatted: Font color: Auto

Formatted: Font color: Auto

Formatted: Font: 12 pt

Formatted: Font: 12 pt, Not Italic

Formatted: Font: 12 pt

Formatted: Font: 12 pt, Not Italic

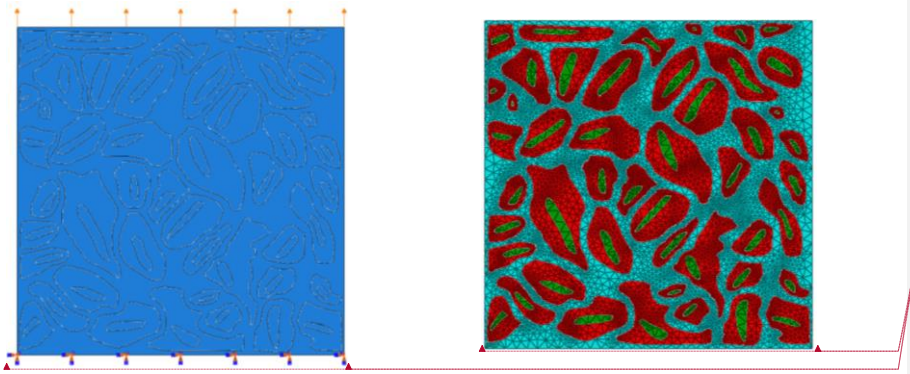

(a) (b)

Figure 3: FE model with the contents of peri phase 61.3% and bee 8.9% (a) Assembled model; (b) FE mesh of bitumen model

As an initial investigation, the materials of the different phases in the bitumen are assumed to be linear elastic. In this study, the Young's modulus of each phase was obtained according to the DMT modulus derived from the AFM device at 20°C. The DMT modulus characterizes materials with significant surface adhesion, which is calculated by summing the load force and adhesive force [36]. Particularly, the Young's moduli of the bee, peri phase and interstitial are 0.000260 N/μm^2, 0.000196 N/μm^2, and 0.000125 N/μm^2, respectively. The selected Poisson's ratio is 0.4.

3 Results and discussion

3.1 Effect of microstructure evolution on the load-bearing capacity of the bitumen

In order to compare the load-bearing capacity of the bitumen with different phases, the external loads derived from the four models are plotted in **Figure 4**.

Formatted: Font color: Auto
Formatted: Font color: Auto
Formatted: Font color: Auto
Formatted: Font color: Auto
Formatted: Font color: Auto
Formatted: Font color: Auto
Formatted: Font color: Auto

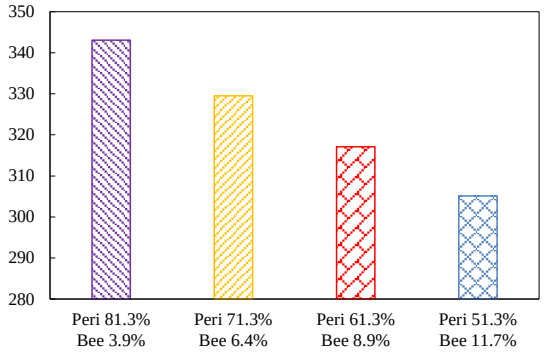

Figure 4: Comparison of the load-bearing capacity of the models with different peri phase and bee contents

The load-bearing capacity increases with combining the increase of the peri phase content and decrease of the bee content, i.e., the bitumen with the contents of peri phase 81.3% and bee 3.9% has the largest load-bearing capacity (0.00343N) and followed by the ones with the contents of peri phase 71.3% and bee 6.4% (0.00329N), the contents of peri phase 61.3% and bee 8.9% (0.00317N) and the contents of peri phase 51.3% and bee 11.4% (0.00305N). However, the difference is not significant and the largest difference is only 11% (between 0.00343N and 0.00305N). Although the Young's modulus of the bee (0.000260 N/μm^2) is larger than those of the peri phase (0.000196 N/μm^2) and the interstitial (0.000125 N/μm^2), the combination of decreasing the contents of the bee and interstitial and increasing the content of peri phase still leads to an increase in the average Young's modulus of the whole bitumen and thus improve the load-bearing capacity.

3.2 Effect of microstructure evolution on distribution of von Mises stress in the bitumen

The distribution of von Mises stress in the FE models is studied in this section. With increasing peri phase content and decreasing the bee content, the higher von Mises stress is distributed mainly in the bee phase, as shown in Figure 5~~Figure 5~~. This phenomenon can be explained by the higher

Formatted: Font color: Auto
Formatted: Font color: Auto
Formatted: Font color: Auto
Formatted: Font color: Auto
Formatted: Font color: Auto
Formatted: Font color: Auto
Formatted: Font color: Auto
Formatted: Font color: Auto
Formatted: Font: 12 pt
Formatted: Font color: Auto

stiffness of bee phase in the microstructure, and hence remarkable stress concentrations usually occur in the bee phases. Although the bee phase decreases in content, the von Mises stress concentration even increases and more stress distributes in the peri phase, which is caused by the decrease of the interstitial content. Consequently, the loads that were previously distributed and dissipated in the interstitial phase will be applied to the other two phases especially to the bee phase. Therefore, it can be deduced that the rejuvenation can effectively improve the load-bearing capacity of bitumen because more stress distributes in the bee and peri phases.

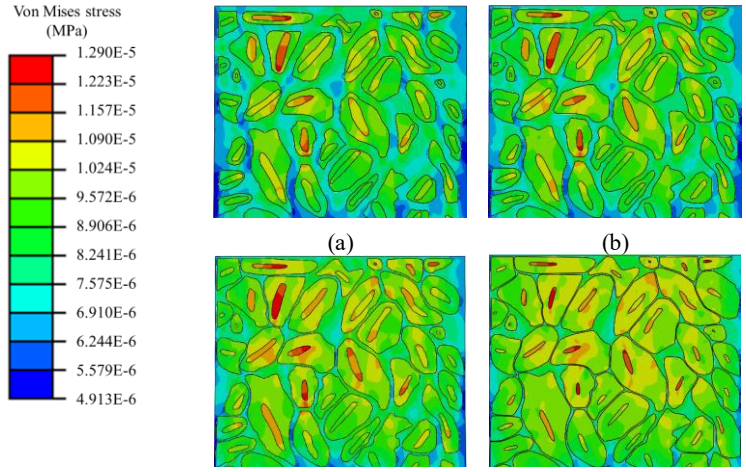

Figure 5: Distribution of the von Mises stress in the sample with (a) peri phase 51.3% and bee 11.4%; (b) peri phase 61.3% and bee 8.9%; (c) peri phase 71.3% and bee 6.4%; (d) peri phase 81.3% and bee 3.9%.

To quantify the distribution of the von Mises stress in the different samples, the cumulative distribution functions (CDFs) are plotted in Figure 6~~Figure 6~~. In probability theory and statistics, the CDF of a real-valued random variable X, evaluated at x, is the probability that X will take a value less than or equal to x [37].

Formatted: Font color: Auto

Formatted: Font color: Auto

Formatted: Font color: Auto

Formatted: Font color: Auto

Formatted: Font: 12 pt

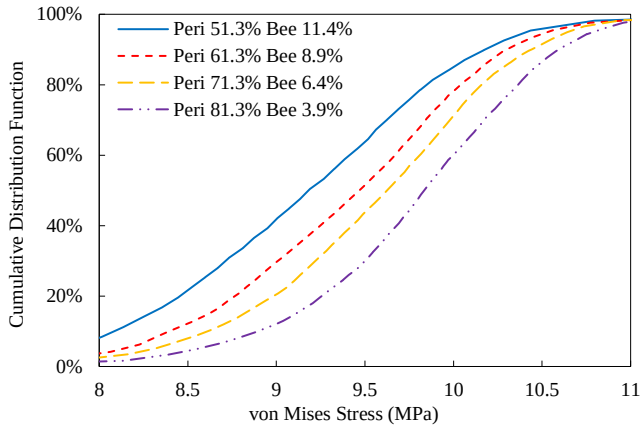
Peri 51.3% Bee 11.4%
Peri 61.3% Bee 8.9%
Peri 71.3% Bee 6.4%
Peri 81.3% Bee 3.9%
Cumulative Distribution Function
100%
80%
60%
40%
20%
0%
8
8.5
9
9.5
10
10.5
11
von Mises Stress (MPa)

(a)

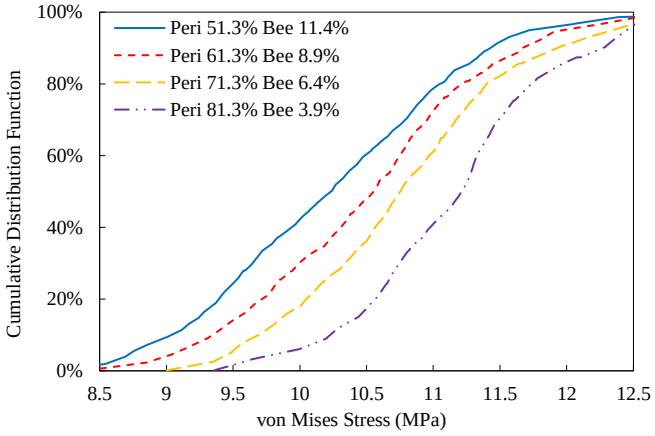
Peri 51.3% Bee 11.4%
Peri 61.3% Bee 8.9%
Peri 71.3% Bee 6.4%
Peri 81.3% Bee 3.9%
Cumulative Distribution Function
100%
80%
60%
40%
20%
0%
8.5
9
9.5
10
10.5
11
11.5
12
12.5
von Mises Stress (MPa)

(b)

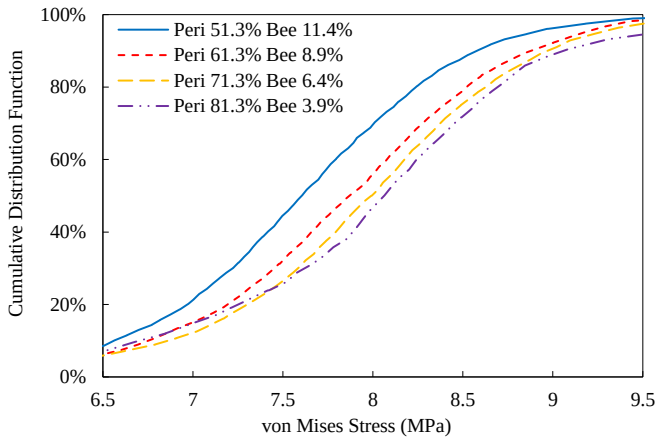

(c)

Figure 6: Cumulative distribution functions of von Mises stress in (a) the peri phase; (b) the bee; (c) the interstitial

These figures show that the percentage of higher von Mises stress increases for every phase in the bitumen samples with an increase of the peri phase content. For instance, in Figure 6~~Figure 6~~ (a) one can see that 80% of the von Mises stress for the sample with 51.3% peri phase and 11.4% bee are at or below 9.85 MPa, and the sample with 81.3% peri phase and 3.9% bee are at or below 10.3 MPa, which leads to a difference of around 0.45 MPa. A similar trend can also be found in the CDFs of the other two phases in Figure 6~~Figure 6~~ (b) and Figure 6~~Figure 6~~ (c). Maximum von Mises stress occurs in the bee phase is larger than those that occur in the other two phases, which is consistent with the observation in Figure 5~~Figure 5~~. One of the more interesting observations from these figures is that the difference in the peri phase is almost equal, and the roughly similar phenomenon can also be found in the bee, while the difference in the interstitial is not, i.e., the distributions of the von Mises stress in the interstitial phase of the bitumen with the three larger peri phase contents are much closer to each other. This may be caused by the fact that the Young's modulus of the bee is around 2.08 times that of the interstitial, and thus the change in the bee content will lead to a more significant

Formatted: Font color: Auto
Formatted: Font color: Auto
Formatted: Font: 12 pt
Formatted: Font color: Auto
Formatted: Font color: Auto
Formatted: Font: 12 pt
Formatted: Font: 12 pt
Formatted: Font: 12 pt
Formatted: Font color: Auto
Formatted: Font color: Auto

difference. Moreover, this phenomenon also indicates that the effects of the bee and peri phase on the anti-damage are greater than that of the interstitial.

The quartile function returns the quartile for a given set of data. Quartile can provide minimum value, first quartile, second quartile, third quartile, and maximum value. As expected, the bee phase exhibits the biggest amount of von Mises stress with a difference in the maximum values of around 0.23 MPa. The difference in the maximum values in the peri phase is 0.10 MPa, which is also expected due to the fact that peri phase exhibits an intermediate stiffness and is more ductile. In conclusion, the stress shows more variations in the bee and peri phases than that in the interstitial phase, which indicates that the bee and peri phases play essential roles in the load-bearing capacity of bitumen.

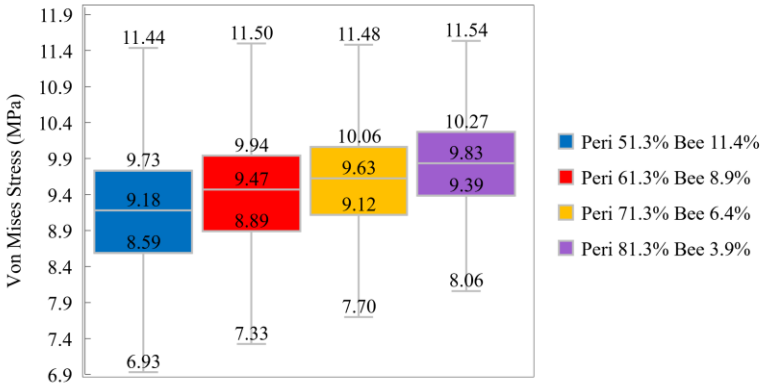

(a)

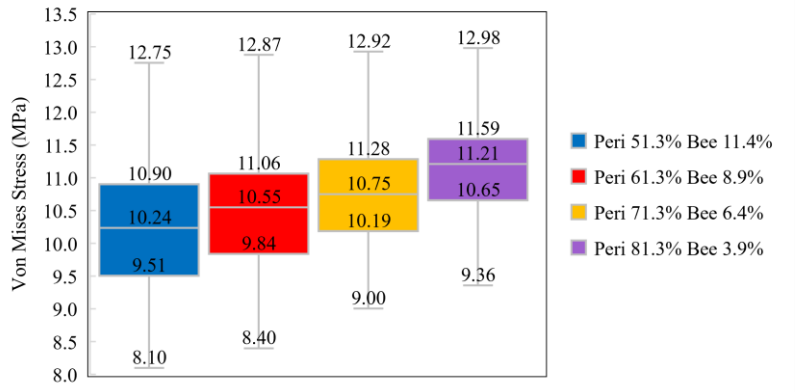

(b)

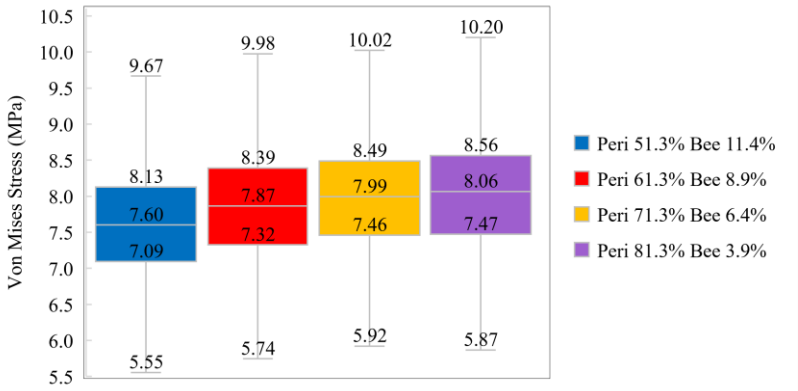

(c)

Figure 7: Quartile Values of von Mises Stress in (a) the peri phase; (b) the bee; (c) the interstitial.

Formatted: Font color: Auto

3.3 Effect of microstructure evolution on the distribution of tensile strain in the bitumen

Formatted: Font color: Auto

Tensile strains in the FE-models with increasing peri phase and decreasing bee content are studied in this section. If a comparison of the tensile strain distribution and concentration between all the models is made, one can see that the patterns of the tensile strain distribution are the same, i.e.,

the higher tensile strain mostly distributes in the interstitial phase of the bitumen due to its lower stiffness, as shown in Figure 8~~Figure 8~~. With the increase of the peri phase content, the distribution of the tensile strain becomes more homogeneous due to more peri phase content which has the intermediate Young's modulus amongst these three phases. Therefore, it can be expected that with the increase of the peri phase, the strain concentrations were remarkably reduced and hence the bitumen will be less vulnerable to the damages.

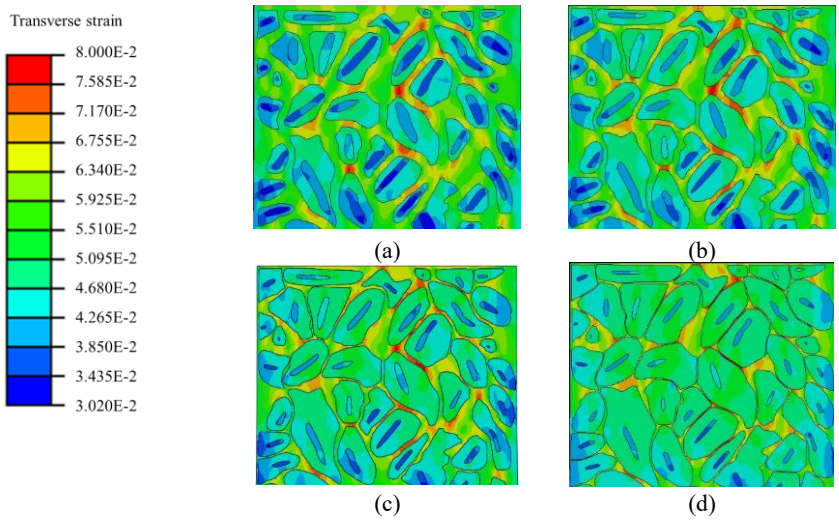

Figure 8: Distribution of the tensile strain in the sample with (a) peri phase 51.3% and B 11.4%; (b) peri phase 61.3% and B 8.9%; (c) peri phase 71.3% and B 6.4%; (d) peri phase 81.3% and B 3.9%.

The CDFs are also plotted in Figure 9~~Figure 9~~ to quantify the distribution of the tensile strain in the different samples. In this figure, one can see a similar trend with that in Figure 6~~Figure 6~~, the percentage of higher tensile strain increases for every phase in the bitumen samples with an increase of the peri phase content. Moreover, the differences in the cumulative distribution between the bitumen with different phases in the peri phase and the bee are almost equal, while the difference in the interstitial is not. The potential reason has been introduced in the last section that the lower stiffness of the interstitial phase causes more strain distributions. It is worth mentioning that the

Formatted: Font: 12 pt
Formatted: Font color: Auto
Formatted: Font color: Auto
Formatted: Font color: Auto
Formatted: Font color: Auto
Formatted: Font color: Auto
Formatted: Font color: Auto
Formatted: Font color: Auto
Formatted: Font: 12 pt
Formatted: Font: 12 pt
Formatted: Font color: Auto
Formatted: Font color: Auto
Formatted: Font color: Auto

maximum tensile strain that occurs in the interstitial is larger than those that occur in the other two phases, while the maximum von Mises stress occurs in the bee phase.

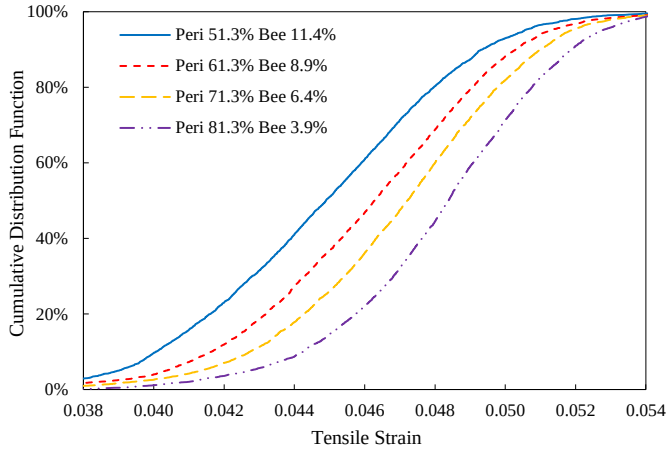

(a)

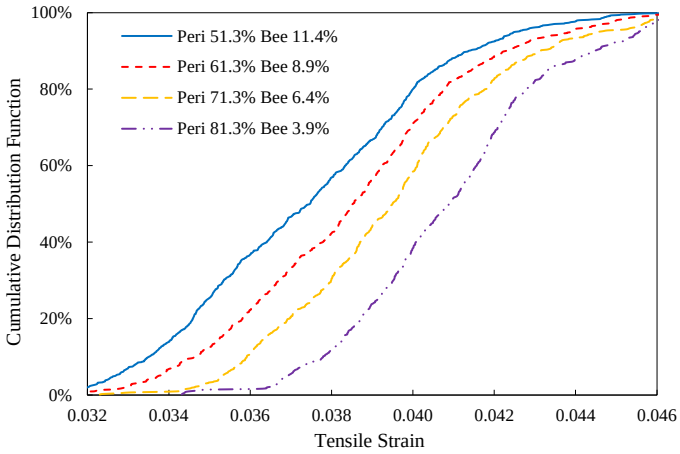

(b)

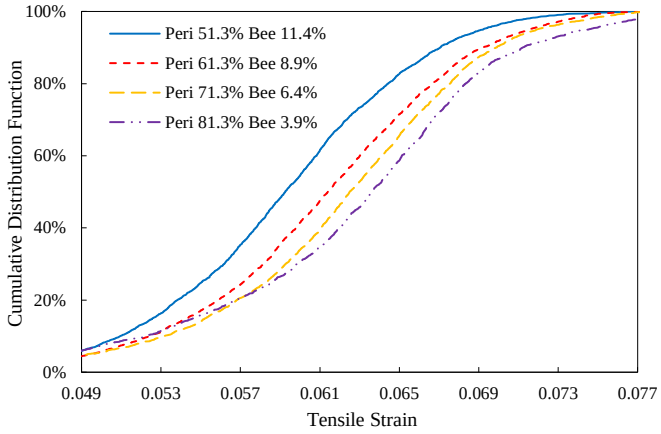

(c)

Figure 9: Cumulative distribution functions of tensile strain in (a) the peri phase; (b) in the bee; (c) the interstitial.

More information about the minimum value, first quartile, second quartile, third quartile, and the maximum value of the tensile strain can be found in Figure 10~~Figure 10~~. This figure further proves the conclusions about Figure 9~~Figure 9~~. The highest strain distributes in the interstitial phase of the bitumen, and less strain variations were observed in this phase, which is consistent with the Quartile Values of von Mises Stress.

Formatted: Font color: Auto

Formatted: Font: 12 pt

Formatted: Font: 12 pt

Formatted: Font color: Auto

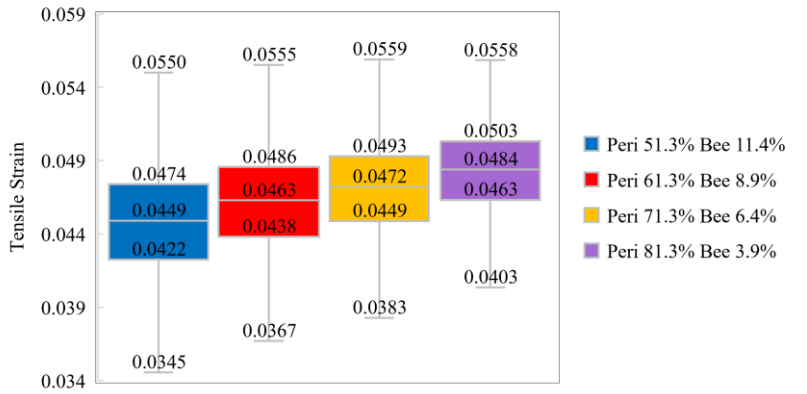
Tensile Strain
0.059
0.054
0.049
0.044
0.039
0.034
0.0550
0.0555
0.0559
0.0558
0.0503
0.0474
0.0486
0.0493
0.0484
0.0472
0.0463
0.0463
0.0449
0.0449
0.0438
0.0422
0.0403
0.0383
0.0367
0.0345
Peri 51.3% Bee 11.4%
Peri 61.3% Bee 8.9%
Peri 71.3% Bee 6.4%
Peri 81.3% Bee 3.9%

(a)

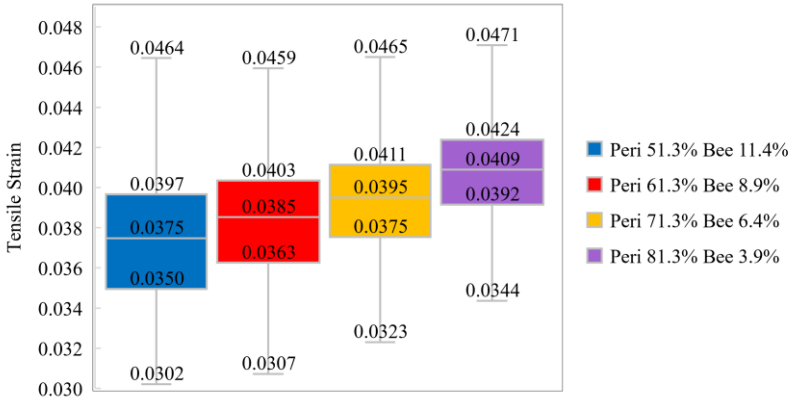
Tensile Strain
0.048
0.046
0.044
0.042
0.040
0.038
0.036
0.034
0.032
0.030
0.0464
0.0459
0.0465
0.0471
0.0424
0.0397
0.0403
0.0411
0.0409
0.0395
0.0392
0.0385
0.0375
0.0375
0.0363
0.0350
0.0344
0.0323
0.0307
0.0302
Peri 51.3% Bee 11.4%
Peri 61.3% Bee 8.9%
Peri 71.3% Bee 6.4%
Peri 81.3% Bee 3.9%

(b)

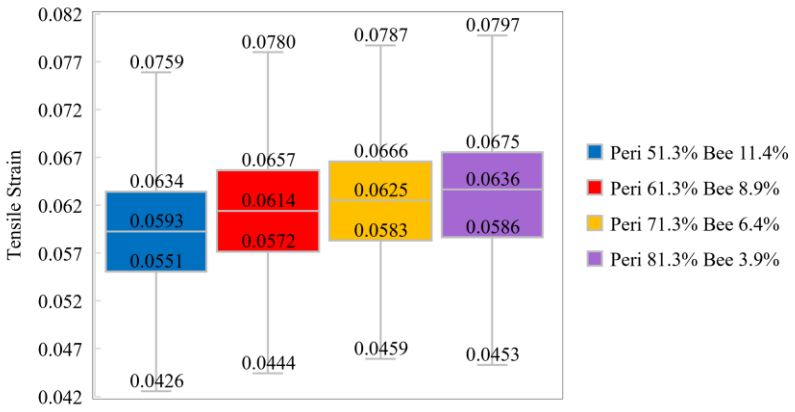

(c)

Figure 10: Quartile Values of tensile strain in (a) the peri phase; (b) the bee; (c) the interstitial.

Formatted: Font color: Auto

4 Conclusions and outlook

The objective of this study was to investigate the effect of the microstructure evolution on the micromechanical property of the bitumen. The interrelationship of the different contents of peri, bee, and interstitial phases of the bitumen and load-bearing capacity, damage nucleation, and tensile strain of the bitumen was evaluated based on FE models. The following conclusions are drawn from the study:

Formatted: Font color: Auto

- The computational load-bearing capacity of the bitumen increases with an increase of the peri phase content. However, the difference is not significant.

Formatted: Font color: Auto

- The higher computational von Mises stress is distributed mainly in the bee phase. With increasing the peri phase content and decreasing the bee content, the von Mises stress concentration increases. This suggests that material inhomogeneity leads to the development of high stresses within the bee phase, which contributes to the damage nucleation and propagation.

Formatted: Font color: Auto

- The higher computational tensile strain mostly distributes in the interstitial of the bitumen. With the increase of the peri phase content, the distribution of the tensile strain becomes more homogeneous.

The aforementioned conclusions indicate that the ability to manipulate the microstructure of bitumen, such as aging and rejuvenation, has a significant influence on the micromechanical properties of the bitumen. However, the effects of the microstructure evolution were identified according to the hypothesized microstructure models, and further researches should be conducted based on the AFM tests on the aged and rejuvenated bitumen. In addition, more research in the future is needed, e.g., to more accurately characterize the micro-material properties of bitumen, and to more accurately and quantitatively assess the relationship between damage evolution in the bitumen and its microstructure.

5 Acknowledgments

This paper is based on a part of the research project carried out at the request of the German Research Foundation, DFG (research project No. FOR 2089/2, OE514/1-2) and Excellence Strategy of the German Federal and State Governments (research project No. StUpPD373-20). The authors are solely responsible for the content.

6 Reference

[1] Eberhardsteiner, L., Blab, R., Design of bituminous pavements - a performance-related approach, Road Materials and Pavement Design 20(2) (2019) 244-258.

[2] Mikhailenko, P., Kou, C., Baaj, H., Poulikakos, L., Cannone-Falchetto, A., Besamusca, J., Hofko, B., Comparison of ESEM and physical properties of virgin and laboratory aged asphalt binders, Fuel 235 (2019) 627-638.

[3] Guo, M., Tan, Y., Interaction between asphalt and mineral fillers and its correlation to mastics' viscoelasticity, International Journal of Pavement Engineering (2019) 1-10.

[4] Romera, R., Santamaría, A., Peña, J.J., Muñoz, M.E., Barral, M., García, E., Jañez, V., Rheological aspects of the rejuvenation of aged bitumen, Rheologica Acta 45(4) (2006) 474-478.

[5] Nayak, P., Sahoo, U.C., A rheological study on aged binder rejuvenated with Pongamia oil and Composite castor oil, International Journal of Pavement Engineering 18(7) (2015) 595-607.

[6] Zaumanis, M., Mallick, R.B., Frank, R., Evaluation of Rejuvenator's Effectiveness with Conventional Mix Testing for 100% Reclaimed Asphalt Pavement Mixtures, Transportation Research Record: Journal of the Transportation Research Board 2370(1) (2013) 17-25.

[7] Zhang, M., Wang, X., Zhang, W., Ding, L., Study on the Relationship between Nano-Morphology Parameters and Properties of Bitumen during the Ageing Process, Materials (Basel) 13(6) (2020).

[8] Wang, D., Falchetto, A.C., Riccardi, C., Westerhoff, J., Wistuba, M.P., Investigation on the effect of physical hardening and aging temperature on low-temperature rheological properties of asphalt binder, Road Materials and Pavement Design (2019) 23.

[9] Loise, Caputo, Porto, Calandra, Angelico, Rossi, A Review on Bitumen Rejuvenation: Mechanisms, Materials, Methods and Perspectives, Applied Sciences 9(20) (2019).

[10] Zhu, X.X., Sun, Y.R., Du, C., Wang, W.Y., Liu, J.Y., Chen, J.Y., Rutting and fatigue performance evaluation of warm mix asphalt mastic containing high percentage of artificial RAP binder, Construction and Building Materials 240 (2020) 11.

[11] Ji, J., Yao, H., Suo, Z., You, Z.P., Li, H.X., Xu, S.F., Sun, L.J., Effectiveness of Vegetable Oils as Rejuvenators for Aged Asphalt Binders, J Mater Civil Eng 29(3) (2017) 10.

[12] Hong, W., Mo, L., Pan, C., Riara, M., Wei, M., Zhang, J., Investigation of rejuvenation and modification of aged asphalt binders by using aromatic oil-SBS polymer blend, Construction and Building Materials 231 (2020).

[13] Guo, M., Liu, H., Jiao, Y., Mo, L., Tan, Y., Wang, D., Liang, M., Effect of WMA-RAP technology on pavement performance of asphalt mixture: A state-of-the-art review, Journal of Cleaner Production 266 (2020).

[14] Howland, R., Benatar, L., A Practical Guide to Scanning Probe Microscopy, (1996).

[15] Butt, H.-J., Cappella, B., Kappl, M., Force Measurements With the Atomic Force Microscope: Technique, Interpretation and Applications, Surface Science Reports - SURF SCI REP 59 (2005) 1-152.

[16] Loeber, L., Sutton, O., Morel, J., Valleton, J.M., Muller, G., New direct observations of asphalts and asphalt binders by scanning electron microscopy and atomic force microscopy, J Microsc-Oxford 182 (1996) 32-39.

[17] Guo, M., Tan, Y., Yu, J., Hou, Y., Wang, L., A direct characterization of interfacial interaction between asphalt binder and mineral fillers by atomic force microscopy, Materials and Structures 50(2) (2017).

[18] Ramm, A., Downer, M.C., Sakib, N., Bhasin, A., Morphology and kinetics of asphalt binder microstructure at gas, liquid and solid interfaces, J Microsc 276(3) (2019) 109-117.

[19] Ramm, A., Sakib, N., Bhasin, A., Downer, M.C., Correlated time-variation of bulk microstructure and rheology in asphalt binders, J Microsc 271(3) (2018) 282-292.

[20] Ramm, A., Sakib, N., Bhasin, A., Downer, M.C., Optical characterization of temperature- and composition-dependent microstructure in asphalt binders, J Microsc 262(3) (2016) 216-25.

[21] Lyne, Å.L., Wallqvist, V., Birgisson, B., Adhesive surface characteristics of bitumen binders investigated by Atomic Force Microscopy, Fuel 113 (2013) 248-256.

[22] Lyne, Å.L., Wallqvist, V., Rutland, M.W., Claesson, P., Birgisson, B., Surface wrinkling: the phenomenon causing bees in bitumen, Journal of Materials Science 48(20) (2013) 6970-6976.

[23] Allen, R.G., Little, D.N., Bhasin, A., Structural Characterization of Micromechanical Properties in Asphalt Using Atomic Force Microscopy, J. Mater. Civ. Eng. 24(10) (2012) 1317-1327.

[24] Allen, R., Little, D., Bhasin, A., Glover, C., The effects of chemical composition on asphalt microstructure and their association to pavement performance, International Journal of Pavement Engineering 15 (2014).

[25] Holleran, I., Masad, E., Holleran, G., Wubulikasimu, Y., Malmstrom, J., Wilson, D.J., Nanomechanical mapping of rejuvenated asphalt binders, Road Materials and Pavement Design (2020) 1-20.

[26] Yang, J., Zhu, X., Yuan, Y., Li, L., Effects of Aging on Micromechanical Properties of Asphalt Binder Using AFM, J. Mater. Civ. Eng. 32(5) (2020).

[27] Cavalli, M.C., Mazza, E., Zaumanis, M., Poulikakos, L.D., Surface nanomechanical properties of bio-modified reclaimed asphalt binder, Road Mater. Pavement Des. (2019) 1-17.

[28] Das, P.K., Baaj, H., Tighe, S., Kringos, N., Atomic force microscopy to investigate asphalt binders: a state-of-the-art review, Road Materials and Pavement Design 17(3) (2015) 693-718.

[29] Chen, A., Liu, G., Zhao, Y., Li, J., Pan, Y., Zhou, J., Research on the aging and rejuvenation mechanisms of asphalt using atomic force microscopy, Construction and Building Materials 167 (2018) 177-184.

[30] Ganter, D., Mielke, T., Maier, M., Lupascu, D.C., Bitumen rheology and the impact of rejuvenators, Construction and Building Materials 222 (2019) 414-423.

[31] Sun, Y.R., Du, C., Zhou, C.H., Zhu, X.X., Chen, J.Y., Analysis of load-induced top-down cracking initiation in asphalt pavements using a two-dimensional microstructure-based multiscale finite element method, Eng. Fract. Mech. 216 (2019) 21.

[32] Liu, P., Hu, J., Canon Falla, G., Wang, D., Leischner, S., Oeser, M., Primary investigation on the relationship between microstructural characteristics and the mechanical performance of asphalt mixtures with different compaction degrees, Construction and Building Materials 223 (2019) 784-793.

[33] Kollmann, J., Liu, P., Lu, G., Wang, D., Oeser, M., Leischner, S., Investigation of the microstructural fracture behaviour of asphalt mixtures using the finite element method, Construction and Building Materials 227 (2019).

[34] Jahangir, R., Little, D., Bhasin, A., Evolution of asphalt binder microstructure due to tensile loading determined using AFM and image analysis techniques, International Journal of Pavement Engineering 16(4) (2014) 337-349.

[35] Luo, D., Macro and micro characterization of reversibility between aging and recycling of asphalt, Harbin Institute of Technology, 2020.

[36] Derjaguin, B., Effect of contact deformations on the adhesion of particles, Progress In Surface Science 45 (1994) 131-143.

[37] Deisenroth, M., Faisal, A., Ong, C., Mathematics for Machine Learning, 2020.